EXCAVATIONS IN SOFT SOILS: REVIEW OF DESIGN APPROACHES

G. Portmann[1], **A. Arnold**[1]

KEYWORDS

Excavations, soft soils, earth pressure, bracing loads, mass displacement, failure mechanisms, numerical modelling, combining practice and theory

ABSTRACT

The design of deep excavations in soft soils is a complex task. Design engineers are typically faced with decisions such as modelling active and passive earth pressures as well as their distribution in terms of bracing loads, the choice of embedment depth of supporting structures with respect to bottom heave and the selected soil-model considered in finite-element codes. The current contribution provides links between these topics in the design of deep excavations in soft soils using the example of an idealised excavation based on selected soil parameters of the "Lilla Bommen" project in soft Gothenburg clay. The modelling of earth pressure distribution is linked to embedment depth and bottom heave as well as to the bracing design. The investigated example of an idealised excavation is analysed with different approaches proposed in literature, allowing for a comparison of earth pressure and bracing load distributions. Subsequently, the excavation is analysed with the finite-element code "Optum G2". Initial results and comparison to analytical models are provided and discussed.

1. INTRODUCTION

Structures in urban areas are increasingly built in and on soft soils. These soils are typically characterised as fine-grained, water-saturated and normally or slightly over-consolidated [1]. Construction in soft soils is challenging as they may respond undrained to changes in load due to a low water permeability. Consequently, excess pore water pressures $\pm\Delta u$ develop, which reduce over time until drained conditions are finally achieved. In the design of an excavation, it is not known a priori whether drained (long-term analysis) or undrained (short-term analysis) conditions are most relevant for the design.

[1] Lucerne University of Applied Sciences and Arts HSLU, School of Engineering and Architecture, Institute of Civil Engineering, Technikumstrasse 21, CH-6048 Horw

Thus, a clear understanding of the development of relevant earth pressures and their effects on the design of an excavation is essential. Various studies on excavations in soft soils [3][7][9][12][13] indicate a correlation between bottom heave stability and loads and/or deformations of the excavation support.

In this article, different design approaches for deep excavations in soft soils are compared on behalf of a case study. An 8 m deep and 40 m wide excavation in soft Gothenburg clay is analysed, (corresponding approx. to the dimensions of the Lilla Bommen tunnel excavation). The focus of the comparative calculation is therefore not to validate the executed "Lilla Bommen tunnel" project, as has been done by other authors. This contribution summarises relevant findings from the first author's master's thesis at HSLU.

2. SUBSOIL

The subsoil data was considered as reported in [8][15]. Gothenburg clay is a slightly over-consolidated (OCR ≤ 2.0), glacial-marine clay. It has a liquid limit of w_L = 76%, a plastic limit of w_P = 34% and an in-situ water content of approx. 55%. The groundwater table is located just below the surface.

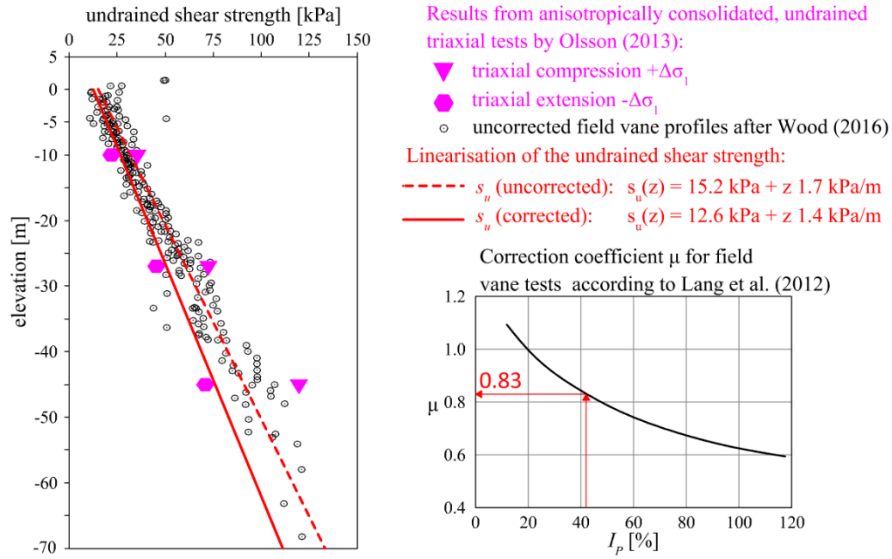

Figure 1 Derivation of an undrained shear strength profile from test data according to Olson [8] and Wood [15].

The subsoil profile was idealised for the calculations as a single layer. Uncorrected soil parameters from field vane shear tests by [15] and the results from undrained triaxial tests on undisturbed soil samples by [8] are summarised in Figure 1. In order to consider the influence of the shear velocity, the s_u-depth profile obtained in field vane shear tests was modified by the correction factor

μ as a function of the plasticity index I_p [6]. The corrected s_u-depth profile is bounded by the results from triaxial compression and extension, however, it correlates more closely to the extension tests. This result is to be expected according to [2] and is believed to provide a suitable basis for the design of an excavation as the majority of the soil experiences a stress change similar to that of triaxial extension (unloading by excavation). The relevant parameters are summarised in Table 1.

Table 1 Geotechnical parameters after [8] and [15]

γ	16.4	kN/m^3	Unit weight
φ'_{cv}	30.5	°	Critical state friction angle
$s_u(z)$	12.6 kPa + z·1.4 kPa/m	kPa	Undrained shear strength profile
k	$4.97 \cdot 10^{-10}$	m/s	Coefficient of permeability
OCR	1.65[1)]	-	Over-consolidation ratio
K_0	0.68[1)]	-	Coefficient of earth pressure at rest
$E_{u,50}$	8.5	MPa	Undrained triax. stiff. at 50% of peak strength
E_{ur}	34.1	MPa	Unloading-reloading Young's modulus
[1)] In-situ measurement by dilatometer testing [15]			

3. RELEVANT DESIGN ASPECTS

Drained or undrained analysis?

Undrained material behaviour is to be expected in low-permeability, fine-grained soils in the event of rapid changes in the loading level, such as arise during excavations. However, the question remains as to whether the consideration of undrained behaviour is relevant for the design of an excavation? Various authors [1][4] report that negative excess pore water pressures (-Δu) must be expected due to the unloading conditions in the predominant area around an excavation pit.

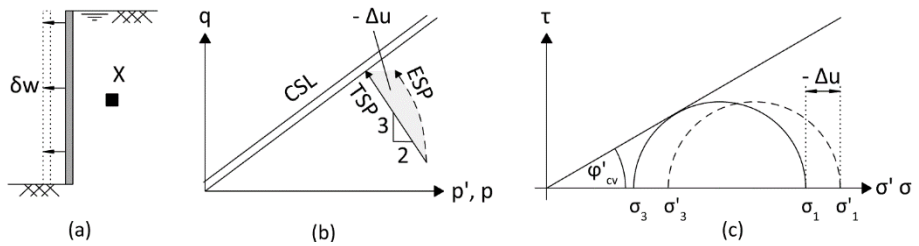

Figure 2 Development of stress paths on the active side of an excavation: (a) Wall displacement leads to unloading on the active side; (b) Effective Stress Path (ESP) and Total Stress Path (TSP) - the ESP reaches the critical state after dissipation of the negative excess pore pressures -Δu; (c) Mohr's stress representation after the excavation with negative excess pore pressures -Δu.

Generally, negative excess pore water pressures either result in higher short-term failure stresses or that the critical state is only reached during consolida-

tion as illustrated in Figure 2. Thus, a free-standing height in the soil may occur in the short term. However, on the basis of this insight and from the consideration of stress paths, it still cannot be concluded that the undrained case with the development of negative excess pore water pressures is not relevant for design. Both the magnitude of the shear stress mobilised at the failure state for a specified water content of the soil and the failure mechanism that occurs is decisive for the analysis.

Bottom heave stability and embedment depth

The bottom heave stability is typically not relevant for soils with $\varphi' \geq 25°$ in the drained state according to [1][13][14]. In undrained conditions, however, this failure mechanism is to be investigated although it may be assumed that negative excess pore water pressures occur in the soil due to the unloading from excavation [1][12][13][14]. Increasing undrained shear strength with depth, as could be observed in the present example, requires that the width of the considered failure mechanism is to be varied so as not to overestimate the stability [1][14]. The calculation approach according to [14] shown in Figure 3(a) and (b) provides a relevant failure mechanism width of $x \cdot B = 7.2$ m for the investigated excavation ($B = 40$ m, $H = 8.0$ m and soil properties according to Table 1). The stability factor F can be defined according to Eq. (1) with the partial safety factors $\gamma_G = 1.20$, $\gamma_Q = 1.30$ und $\gamma_{GB} = 1.30$ [1].

$$F = \frac{\frac{1}{\gamma_{GB}}\left(R_{v,k} + R_{GB,k}\right)}{\gamma_G \cdot G_k + \gamma_Q \cdot Q_k} \tag{1}$$

The forces are defined as (see also Figure 3)

$$R_{GB,k} = 5.14 \cdot s_{u2} \cdot x \cdot B;\ R_{v,k} = s_{u1} \cdot H;\ G_k = \gamma \cdot H \cdot x \cdot B;\ Q_k = q_k \cdot x \cdot B \tag{2}$$

and the bottom heave stability is assumed to be sufficient for values $F \geq 1.0$. In the excavation under consideration, a value of $F = 0.79$ results at design level, indicating insufficient bottom heave stability.

Methods for increasing bottom heave stability reported in [13] consist of: (I) Increasing the embedment depth *t;* (II) Increasing the load within the excavation pit (e.g. underwater excavation); (III) Creating a supporting base slab / jetting slab before excavation begins; (IV) Reducing the effective excavation depth by removing soil in a sufficiently large area next to the excavation pit; or (V) Excavating a series of smaller pits. In this way, spatial effects may be mobilised and a greater bearing capacity factor N_c would result [11].

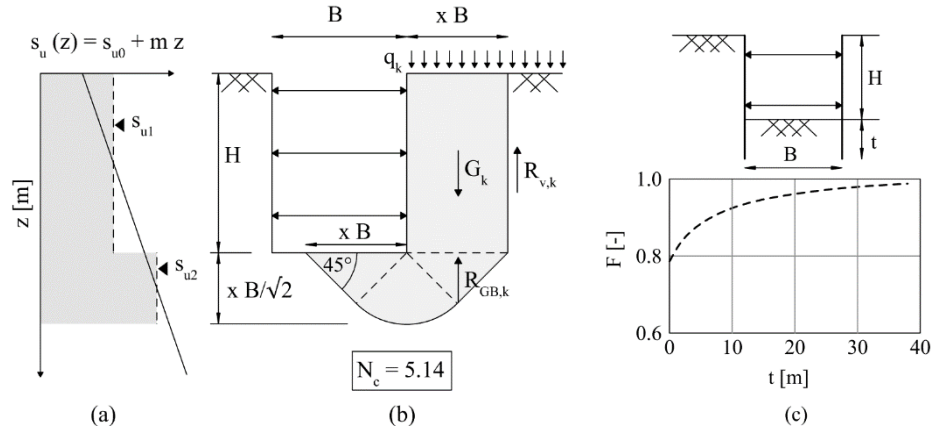

Figure 3 Calculation of the bottom heave stability for $s_u(z) \neq$ const. and variable width x B: (a) s_u-profile; (b) Approach according to Weissenbach and Hettler [14] with a load-bearing capacity factor $N_c = 5.14$; (c) Influence of the embedment depth t on the factor of safety F.

Increasing the embedment depth *t* in order to improve the bottom heave stability as a seemingly simple and cost-effective measure is the subject of controversial debate. This can be shown by way of example with the approach according to [14] as formulated in Eq. 1. In the present investigation, even for very large embedment depths of $t > 20$ m, the calculated level of safety does not fulfil the requirements, see Figure 3(c). It is assumed that the bottom heave failure mechanism develops below the embedment depth as shown in Figure 4(a).

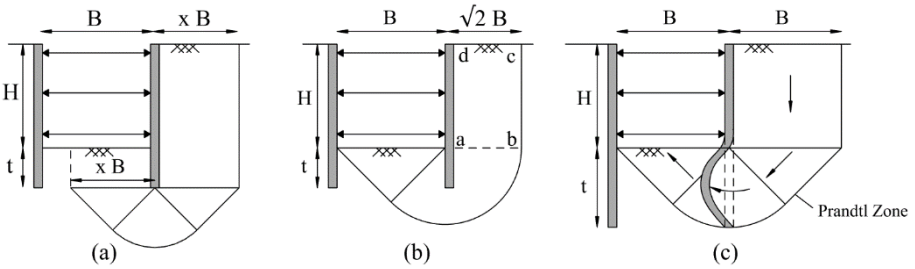

Figure 4 Influence of the embedment depth t on the bottom heave stability mechanism: (a) The mechanism develops below t [14]; (b) t only influences the mechanism if $t > \sqrt{2}$ B [9]; (c) Dowel effect of the embedment depth [7].

Some other design approaches also imply that large embedment depths are necessary to influence the relevant failure mechanism and thus improve the bottom heave stability [9], see Figure 4(b). In contrast there are approaches that consider dowel action over the embedment depth [3][7], as illustrated in Figure 4(c), whereby in [13] it is suggested that the forces required to retain the soil are transferred upwards in the case of stiff excavation closures, leading to significantly higher bracing forces.

The influence of bottom heave stability is viewed critically as described in [12][13] for another reason. Terzaghi et al. (1996, p.307, [12]) provide the following description: "If the underlying clay experiences a bearing-capacity failure, the bottom of the excavation heaves and the earth pressure against the bracing increases dramatically". This is portrayed in [12] with a larger failure mechanism as seen in Figure 5 for $F < 1.0$.

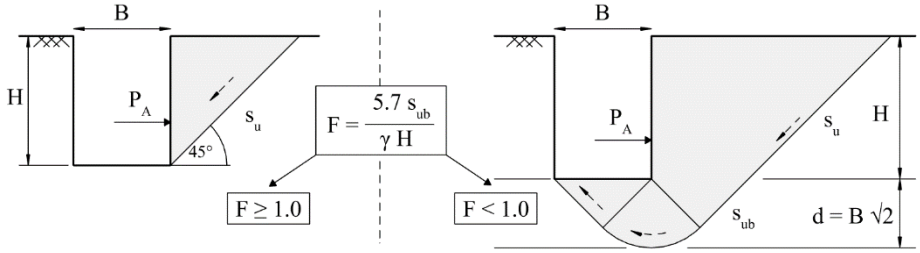

Figure 5 Possible failure mechanism for excavations with bottom heave (F < 1) and without (F > 1) after [12].

As the requirement for bottom heave stability cannot be satisfied in the current example, a grouted base slab should be constructed before excavation. This construction sequence is generally recommended for excavations in soft soils with depths greater than 5 m [1]. The grouted base slab has the following functions: (I) Creating a base support to ensure the equilibrium of the horizontal forces; (II) Minimising the deformations of the excavation pit support in the foot area in order to limit the settlements outside the excavation pit; and (III) Securing the excavation pit against bottom heave and buoyancy.

The proposed grouted base slab is to be constructed with a thickness of 2 m from -9.0 to -11.0 m, the embedment depth of the diaphragm wall amounts to $t = 4$ m, see Figure 6(a). The grouted base slab must also be secured with tension piles. Possible design approaches are described in [1][14].

Earth pressure and bracing forces

The earth pressures and bracing forces are determined analytically and numerically for the excavation illustrated in Figure 6(a). To allow direct comparison with FEM results, characteristic earth pressures are given.

Earth pressure at rest

Excavation pit supports with prestressed bracings in the upper region and a base support constructed prior to the start of excavation are assumed to be sufficiently rigid so that the earth pressure at rest can be accounted for in the design [1]. Hence, undrained conditions are not considered and earth pressures are calculated as shown in Figure 6. The following aspects should be addressed:

- As a simplification, no passive earth pressure is considered within the excavation – the grouted base slab is activated as a support, see Figure 6(b).

- Earth pressure at rest is considered with a value of $K_0 = 0.68$, as determined in the subsoil investigation (Table 1).

$$e'_{0p,k} = K_0\, p_k = 6.8 \text{ kPa};\; e'_{0,k} = K_0\, \gamma' z = 52.2 \text{ kPa};\; u_k = \gamma_w\, z = 120 \text{ kPa} \quad (3)$$

- A degree of earth pressure redistribution is to be considered for prestressed bracings. This can be accounted for in a simplified manner by increasing the resulting support forces by 30% [1]. Hence, the bracing force N_k is calculated from the upper support force, see Figure 6(c), and increased by 30% for the spacing of $a = 5$ m:

$$N_k = 1.3\ (5 \text{ m})\ 252\,\frac{\text{kN}}{\text{m}} = 1'640 \text{ kN} \quad (4)$$

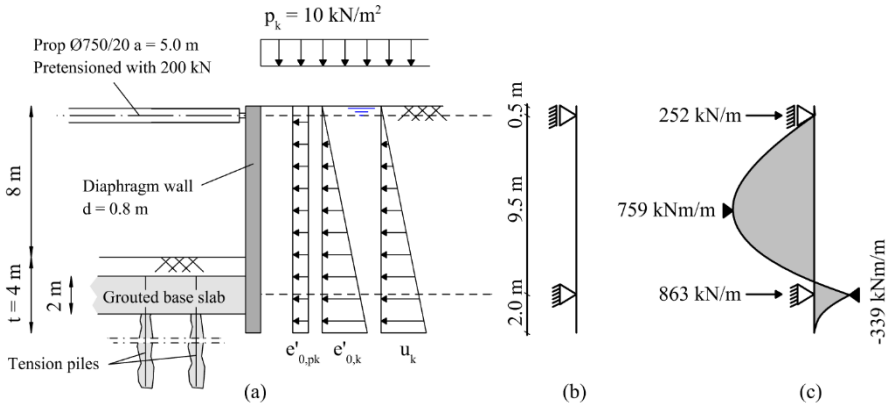

Figure 6 Earth pressure at rest: (a) Actions; (b) Simplified static system; (c) Support reactions and moment distribution.

Total stress analysis

The active earth pressure may be calculated for the undrained case, neglecting the influence of wall friction:

$$e_{ak} = p_k + \gamma\, z - 2\, s_u(z) = 148 \text{ kPa} \quad \text{for } z = 12 \text{ m} \quad (5)$$

It is assumed that cracks could form due to tensile stresses up to a height of h_{cr}. When such cracks are filled with water, hydrostatic water pressure takes effect.

$$h_{cr} = \frac{-(2\, s_{u0} - p_k)}{2\, m - \gamma} = 1.12 \text{ m with } s_{u0} = 12.6 \text{ kPa and m} = 1.4 \text{ kPa/m} \quad (6)$$

In the case of passive earth pressure, it is assumed that the grouted base slab and the soil above act as a surcharge load with a pressure of 56 kPa.

$$e_{pk1} = 56 \text{ kPa} + 2\, s_u(11\text{m}) = 112 \text{ kPa} \quad (7)$$

$$e_{pk2} = 56 \text{ kPa} + \gamma\ 1\text{m} + 2\, s_u(12\text{m}) = 131 \text{ kPa} \quad (8)$$

The earth pressure distribution and resulting moment distribution are illustrated in Figure 7. Subsequently, the bracing force can be calculated at a horizontal spacing of a = 5 m. As before, a degree of earth pressure redistribution is taken into account by increasing the resulting support force by 30%.

$$N_k = 1.3\ (5\ \text{m})\ 163\frac{\text{kN}}{\text{m}} = 1'060\ \text{kN} \qquad (11)$$

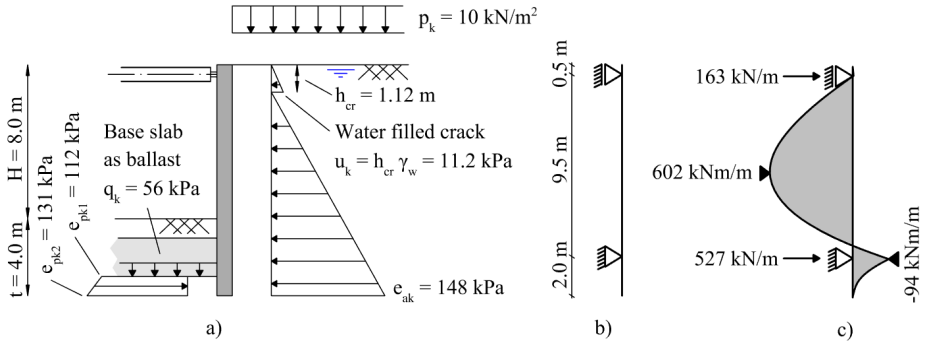

Figure 7 Total stress analysis: (a) Actions; (b) Simplified static system; (c) Support reactions and moment distribution.

Bracing force diagrams

The critical bracing forces activated across all construction stages may also be estimated using apparent earth pressure diagrams according to Terzaghi et al. [12] or based on Distributed Prop Load (DPL) diagrams according to Twine and Roscoe [13], see Figure 8.

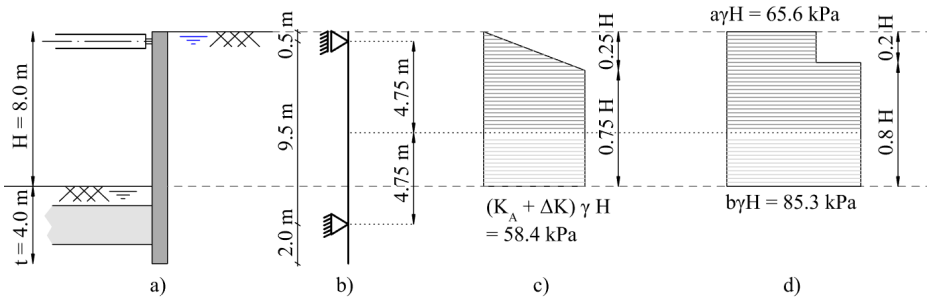

Figure 8 Estimation of maximum bracing force: (a) Excavation pit; (b) Static system; (c) Apparent earth pressure diagram according to Terzaghi et al. [12]; (d) Distributed prop load diagram (DPL) according to Twine and Roscoe [13].

In the investigated case, a jet grouted base slab is constructed as a base support before excavation begins and is secured with tension piles. Thus, it is not assumed that a significant force redistribution results in the bracings from the failure mechanism shown in Figure 5. In the approach according to Terzaghi et al. [12], this results in a value of $\Delta K = 0$. Subsequently, the value of K_A can be calculated for $s_u(H/2)$ = 18.2 kPa, shown in Figure 8, as follows:

$$K_A = 1 - \frac{4\, s_u}{\gamma H} = 0.445 \quad (9)$$

According to the approach proposed by Twine and Roscoe [13], the DPL is applied as illustrated in Figure 8(d), which is independent of the undrained shear strength. For the case not at risk of bottom heave, the coefficients result to $a = 0.5$ and $b = 0.65$.

The bracing forces are calculated considering half the distance between the supports as is indicated by the dashed line in Figure 8. Hence, a bracing force of N_k = 1'241 kN results according to Terzaghi et al. [12], whereas N_k = 2'080 kN according to the approach by Twine and Roscoe [13].

FEM

An undrained, elastoplastic FEM analysis was performed for the current investigation. Structural components such as the diaphragm wall, jetting base and anchors were modelled as wished in place in accordance with [10]. Subsequently, the continued excavation was simulated in 1.5 – 2 m depth increments. The calculations were performed in OPTUM G2 with an axially symmetric model, dimensions of b = 120 m and h = 70 m and an automatically refined FE-mesh consisting of 3'000 elements of type 6-node Gauss. The soil-structure stiffness ratios and the friction mobilised between the soil and the structural component have a significant influence on the development of the deformations and the earth pressures: The diaphragm wall was modelled with a flexural stiffness $EI^{II} = 27.23\ 10^4$ kNm^2/m; the interface-reduction factor was taken as 0.5; the bracing was considered with an axial stiffness EA = $96.32\ 10^5$ kN and prestressing force of 200 kN at a spacing of a = 5 m; the grouted base slab was modelled with E = 1'800 MPa, v = 0.2 as for concrete and c = 2.5 N/mm^2, $\varphi' = 0°$ with the Mohr-Coulomb material model. It could be shown that the interface between the base slab and the diaphragm wall has a significant influence on the load-deformation behaviour. The model simulates an incomplete interface between the grouted base slab and the diaphragm wall by considering a reduced wall friction up to a maximum of 50% in relation to the surrounding soil.

Table 2 Input parameters for the soil material models.

Material Model		11 Tresca	12 Tresca	AUS PEAK	AUS ENTF
$E_{u,50}$	[MPa]	8.5	34.1 ≈ E_{ur}	-	-
E_u	[MPa]	-	-	85	85
$\varepsilon_{c,50}$	[%]	-	-	0.28	0.28
$\varepsilon_{e,50}$	[%]	-	-	0.47	0.47
$s_u(z)$	[kPa]	12.6+z·1.4	12.6+z·1.4	9.4+z·2.43	11.6+z·1.54
s_{ue}/s_{uc}	[-]	-	-	0.61	0.61
Tension Cut-Off	[-]	Yes	Yes	Yes	Yes
γ_{sat}	[kN/m^3]	16.4	16.4	16.4	16.4
K_0	[-]	0.68	0.68	0.68	0.68

Two undrained material models were implemented to simulate the soil behaviour (total stress analysis), namely, the linear elastic - ideal plastic Tresca and the elasto-plastic AUS (Anisotropic Undrained Shear) soil model [5]. The input parameters were calibrated using a triaxial test according to [8] as summarised in Table 2, resulting in the stress-strain curves shown in Figure 9.

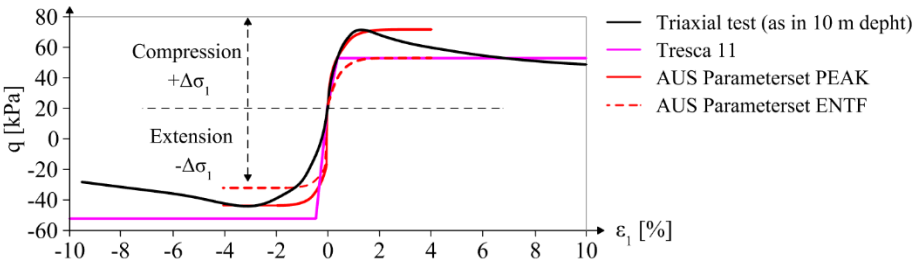

Figure 9 Calibration of the material models using two triaxial tests according to [8] to represent a stress level at a depth of 10 m.

The FE analyses resulted in the earth pressure distributions as illustrated in Figure 10. In addition to the resulting earth pressures, the earth pressure at rest and the total active and passive earth pressures are also shown.

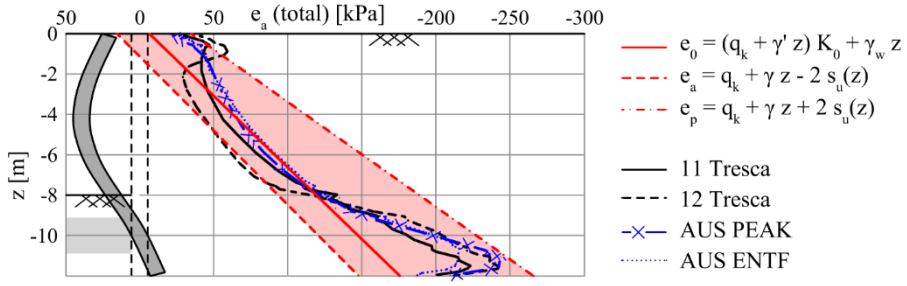

Figure 10 Comparison of mobilised earth pressures resulting from FEM calculations with those from a total stress analysis. Wall deformations are indicated overdrawn.

4. COMPARISON OF RESULTS AND CONCLUSIONS

The results from the FE-analysis indicates that the earth pressures react sensitively to the stiffness characteristics in the model as is shown in Figure 10. Consequently, an earth pressure ranging between the earth pressure at rest and the active earth pressure could be mobilised between the bracing and the grouted base slab as a function of the stiffness ratio between the subsoil and diaphragm wall (Tresca 11 & 12). Furthermore, the diaphragm wall appears to rotate around a point approximately at the height of the middle of the base slab. This resulted in the activation of nearly passive earth pressures outside the excavation within the bottom region of the diaphragm wall. Moreover, the analysis indicates a redistribution of forces from the free span length in the direction of the pre-stressed bracings. Figure 11 provides a comparison of the bracing forces and the maximum span moments obtained from the analytical

and numerical calculations. The following three effects could be observed:
(I) The approach considering earth pressure at rest (drained) appears to result in a safe design for the present investigation, only the approach according to Twine and Roscoe [13] resulted in higher bracing forces, although their diagram is based on multiple-propped excavations in which the greatest bracing forces are known to occur before the next layer of bracings are installed;
(II) The total earth pressure approach (± 2 s_u) seemingly results in an underestimation of the bracing force, especially if no increase of 30% due to earth pressure redistribution is taken into account whereas the approach according to Terzaghi et al. [12] compares favourably with the numerical calculations;
(III) The analytical calculations result in higher bending moments than the numerical analyses.

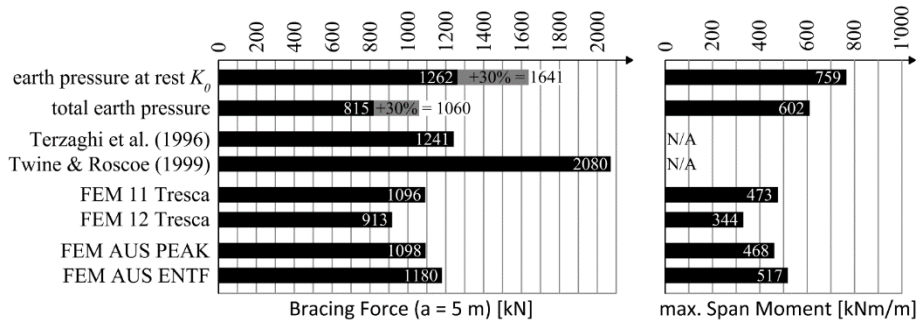

Figure 11 Comparison of the bracing forces and the maximum span moments from the analyses.

The following conclusions could be drawn from the current investigation: For deep excavations in soft soils, there is a risk of bottom heave and large deformations outside the excavation due to ground displacements associated with heave of the excavation base. Thus, the construction practice recommendation that a base support should be provided for excavations in soft soils with $H > 5$ m before the start of excavation [1] seems appropriate. An overview of literature on the subject and the example calculations indicate that the influence of the embedment depth remains controversial. Insight into the complex soil-structure interaction and activated earth pressure distributions can be obtained through FE-analysis. Interestingly, even the relatively simple, linear elastic - ideally plastic Tresca soil model provides similar results to the elasto-plastic AUS soil model with regard to the earth pressure distribution. However, such simple material models are less appropriate in the investigation of deformations around an excavation [10] as they typically do not distinguish between initial and un/reloading in terms of stiffness. A FE-analysis of the undrained conditions with an effective material model (modified cam clay or similar) was not performed. In order to mitigate the risk of unsafe design, the degree of mobilised shear strength must be verified by field measurements for analyses where the undrained shear strength is a result of the material model and not an input parameter.

REFERENCES

[1] Deutsche Gesellschaft für Erd- und Grundbau Arbeitskreis Baugruben: Empfehlungen des Arbeitskrieses Baugruben EAB, 6th ed. Berlin: Wilhelm Ernst & Sohn, 2021.

[2] A. Hettler, S. Leibnitz, and F. Biehl: Zur Kurzzeitstandsicherheit bei Baugrubenverbaukostruktion. in weichen Böden. Bautechnik, vol. 79, 2002.

[3] M. Huang, Z. Tang, and J. Yuan: Basal stability analysis of braced excavations with embedded walls in undrained clay using the upper bound theorem. TUST, vol. 79, 2018.

[4] H.-G. Kempfert and B. Gebreselassie: Excavations and foundations in soft soils. Berlin: Springer-Verlag, 2006.

[5] K. Krabbenhoft, A. Lymain, and J. Krabbenhoft: OPTUM G2: Materials, 2016

[6] H.-J. Lang, J. Huder, P. Amann, and A. M. Puzrin: Bodenmechanik und Grundbau: Das Verhalten von Böden und Fels und die wichtigsten grundbaulichen Konzepte, 9th ed. Berlin Heidelberg: Springer, 2011.

[7] T. D. O'Rourke: Base stability and ground movement prediction for excavations in soft clay. London: Thomas Telford, 1993.

[8] M. Olsson: On Rate-Dependency of Gothenburg Clay. Doctoral Thesis, Chalmers University of Technology, Göteborg, Sweden, 2013.

[9] C.-Y. Ou: Deep Excavation - Theory and Practice. London: Taylor & Francis, 2006.

[10] D. Potts, K. Axelsson, L. Grande, H. Schweiger, and M. Long: Guidelines for the use of advanced numerical analysis. London: Thomas Telford, 2002.

[11] A. W. Skempton: The bearing capacity of clays, in Proceedings of Building Research Congress Vol.1, 1951.

[12] K. Terzaghi, R. B. Peck, and G. Mesri: Soil Mechanics in Engineering Practice, 3rd ed. New York: Wiley, 1996.

[13] D. Twine and H. Roscoe: Temporary propping of deep excavations - guidance on design. CIRIA publication C517. London: Construction Industry Research and Information Association, 1999.

[14] A. Weissenbach and A. Hettler: Baugruben Berechnungsverfahren. 2nd ed. Berlin: Ernst & Sohn, 2011.

[15] T. Wood: On the small strain stiffness of some Scandinavian soft clays and its impact on deep excavations. Doctoral Thesis, Chalmers, Göteborg, Sweden, 2016.